

# Sparrow Time Series Data Analysis

**Sara Capdevila Solé, CID: 01727810**

Supervisor: Tim Evans

Assessor: Kim Christensen

Word Count: 6376

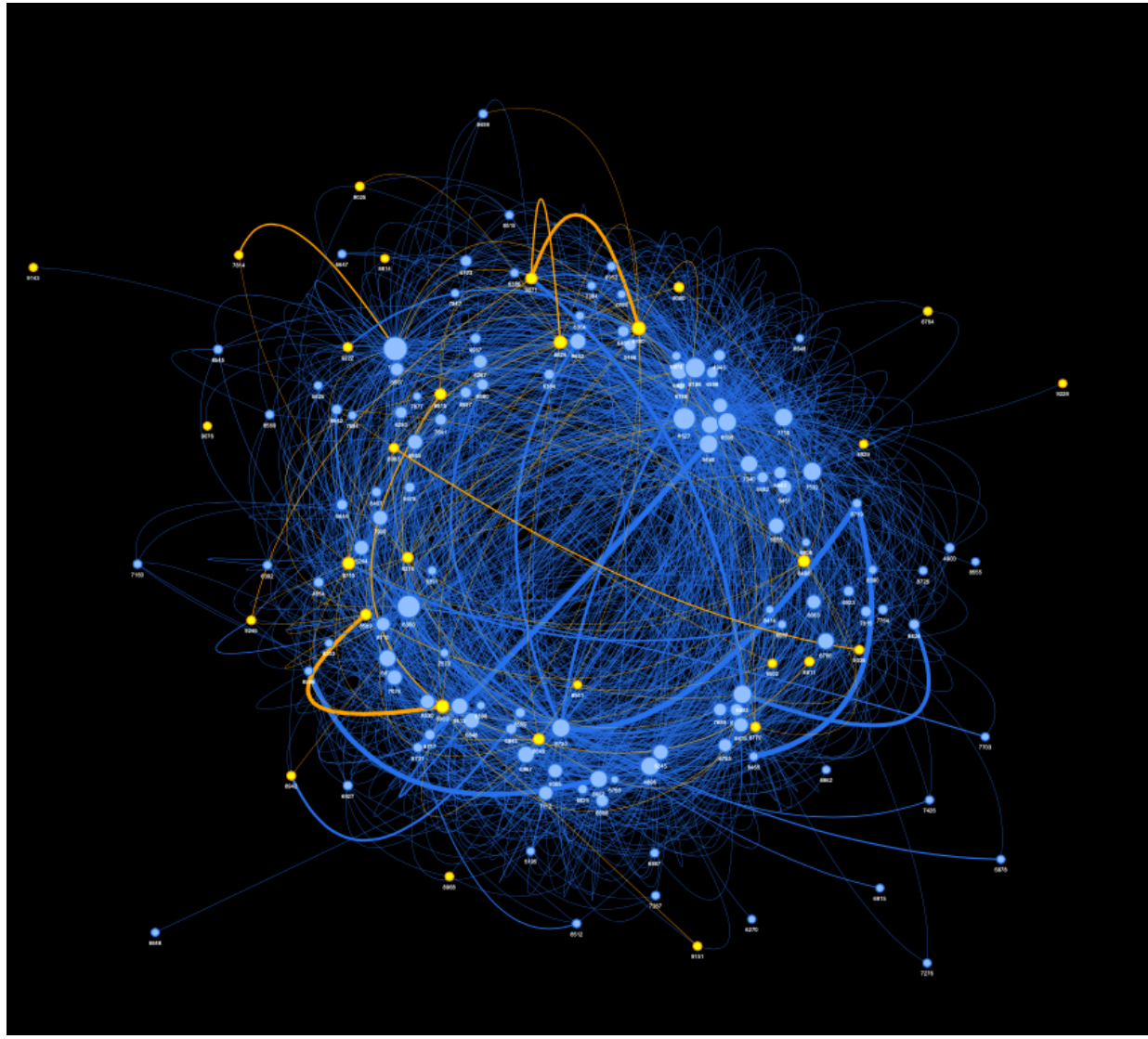


Fig. 1: **Sparrows network:** “Spaghetti Monster” network of birds given certain ‘interaction’ criteria. A figure that does not convey any useful information [1]. Visualisation created using *Pyvis* [2].

Department of Physics, Blackett Laboratory

Imperial College London

London, United Kingdom

06/05/2022

CONTENTS		
<b>I</b>	<b>Introduction</b>	2
<b>II</b>	<b>Data acquisition</b>	2
<b>III</b>	<b>Data Overview</b>	2
<b>IV</b>	<b>Theory - The making of a network</b>	3
IV-A	Landing times: "Alpha" ( $\alpha$ ) . . . . .	3
IV-B	Establishing Social Connections: "Beta" ( $\beta$ ) . . . . .	3
<b>V</b>	<b>Network analysis</b>	4
V-A	Average shortest path length . . . . .	4
V-B	Eccentricity . . . . .	4
V-C	Community detection . . . . .	4
V-D	Centrality as a Measure of Sociability . . . . .	4
V-D1	Betweenness . . . . .	4
V-D2	Closeness . . . . .	4
V-D3	Eigenvector . . . . .	4
<b>VI</b>	<b>Looking for alpha and a beta</b>	4
VI-A	Bird patterns . . . . .	4
VI-B	Variation in network measures . . . . .	5
VI-C	Empirical considerations . . . . .	5
<b>VII</b>	<b>Correlations</b>	5
<b>VIII</b>	<b>Powers laws</b>	6
<b>IX</b>	<b>Sparisification Methods</b>	7
IX-A	Weakest connection . . . . .	7
IX-B	Edge threshold . . . . .	7
IX-C	L-score . . . . .	7
IX-D	Expected connections . . . . .	7
IX-E	Repeated connections . . . . .	8
IX-F	Network variation . . . . .	8
IX-F1	Ratio of kept edges . . . . .	8
IX-F2	Eccentricity and shortest path length . . . . .	8
<b>X</b>	<b>Repeatability</b>	9
<b>XI</b>	<b>Jaccard Similarity</b>	9
XI-A	Node comparison . . . . .	9
XI-B	Edge comparison . . . . .	10
<b>XII</b>	<b>Describing our network</b>	10
XII-A	Threshold comparison: most significant connections . . . . .	10
XII-B	Comparison: weeks and seasons . . . . .	10
XII-C	Flock size: Community detection . . . . .	10
<b>XIII</b>	<b>Simulated networks</b>	11
XIII-1	Method 1 - Conserve Bird Landing Number . . . . .	11
XIII-2	Method 2 - Don't Conserve Bird Landing Number . . . . .	11
	XIII-3 Method 3 - Distribute Bird Landing Numbers . . . . .	11
	XIII-A Comparison . . . . .	12
<b>XIV</b>	<b>A brief look into dominance at the feeder</b>	13
XIV-A	Elo ranking . . . . .	13
XIV-B	Sex-dominance relationship . . . . .	13
<b>XV</b>	<b>Discussion and conclusions</b>	14
	<b>Appendix A: Network analysis</b>	14
	<b>Appendix B: Network dimensions</b>	14
	B-A Average shortest path length . . . . .	14
	B-B Eccentricity . . . . .	14
	B-C Community detection - maximising modularity . . . . .	15
	<b>Appendix C: Centrality measures</b>	15
	C-A Betweenness . . . . .	15
	C-B Closeness . . . . .	15
	C-C Eigenvector . . . . .	15
	<b>Appendix D: P-values and <math>\chi^2</math>-test</b>	15
	<b>Appendix E: Network structure variation</b>	15
	<b>References</b>	15

## Abstract

In this report, we analyse and visualise networks from a time series RFID data, obtained from a sparrow feeder in Lundy Island. We have introduced temporal parameters to identify sparrows' landings, and how they form connections. In this investigation, we propose different network sparsification methods to extract the most important sparrow connections. With this, we also identify a list of the top 10 most dominant sparrows in the feeder. Furthermore, we analyse centrality measures, network dimensions and communities. As expected, we find a high average correlation of 0.68 between network centrality measures (betweenness, closeness and eigenvector, as well as total network edges and average node degree), with a standard deviation of 0.26. Additionally, we look at Jaccard similarity methods, and centrality correlations to compare two different networks. This has allowed us to extract the mean weekly repeatability of connections of 2 weeks and 2 days with a margin of error of  $\pm 4$  days, at a 95% significance level. We compare our network to 100 trials of 3 different simulated random networks. We find that it's very unlikely to find a similar friendship repetition of  $> 2$  weeks, that can be replicated randomly, with a  $p$ -value of  $< 1\%$ . Additionally, centrality measures were found to be significantly different with a minimum mean  $p$ -value of  $0.012 \pm 0.005$ . Finally, we propose further improvements to this investigation.

## I. INTRODUCTION

**S**PARROWS are small brown birds, very predominant in most of the European territory. They are known to be social animals, and cohabit in clusters of organized groups, called flight flocks [3].

Their behaviour and social tendencies are not well understood yet. Understanding these can give ornithologists insight into why population changes occur seasonally when factors such as competition, predation, diseases, and agricultural practices are controlled [4]. Sparrows are a significant part of the food chain in our ecosystem - they are a source of food for other animals higher in the chain and also help in the reproduction and survival of plants by spreading seeds as they feed on their products, such as fruits.

Social structures, groupings and bird personality traits, as well as dominance, have been thoroughly ecologically investigated [5][6][4]. However, we use these insights to approach these questions through an analysis of networks. Additionally, this analysis also provides an opportunity to investigate and explore network measures and their variations under different conditions, and periods of the year.

## II. DATA ACQUISITION

Lundy Island is a small Island off the North Devon coast of the UK. A project of interest on this Island is the investigation of the behaviour of a population of sparrows [5]. These birds are each harmlessly tagged with a unique Radio-frequency identification (RFID) chip [7] on their leg.

This study is focused on recordings of these RFID chips at a sparrow feeder on the Island. Sparrow data at a feeder can establish connections between birds, as members who stay in close spatial proximity [8], or who synchronize activities such as foraging, can be considered to be in the same social grouping [9] [10]. These characteristics all form basic elements of the social structure of species, and are associated with important fitness consequences in group-living animals [11].

A picture of the sparrow feeder in Lundy Island with the RFID hardware and sparrows is shown in Fig. 2. a and b, respectively.

## III. DATA OVERVIEW

Data consists of bird ID and time for each second it is detected at the feeder. The data spans two different winter seasons. The first season ranges from [01.11.2015, 31.01.2016] and comprises 118 different birds. The range of the second



(a) **Sparrow feeder:** with sparrows and the RFID detection hardware.  
(b) **Sparrow:** with an RFID tag attached to their leg.

Fig. 2: **Sparrow and the sparrow feeder in Lundy Island:** Bird presence is recorded using the RFID system setup. Depending on their landing time, information on their social behaviour can be extracted and networks can be created.

season is similar, from [04.11.2016, 31.01.2017] with a smaller set of only 69 birds. There are 37 birds that appear in both seasons.

The data has approximately  $4.1 \times 10^5$  readings of birds landing through both seasons. These are non-uniformly distributed throughout each of the seasons. The first season makes up for 70% of these recordings.

The distribution of RFID readings in the feeder throughout the seasons is plotted in Fig. 3.

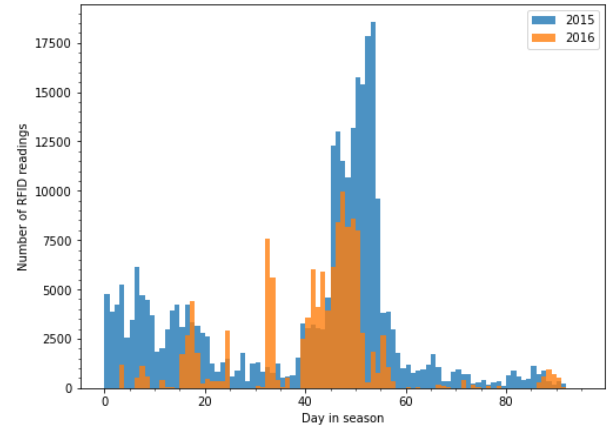
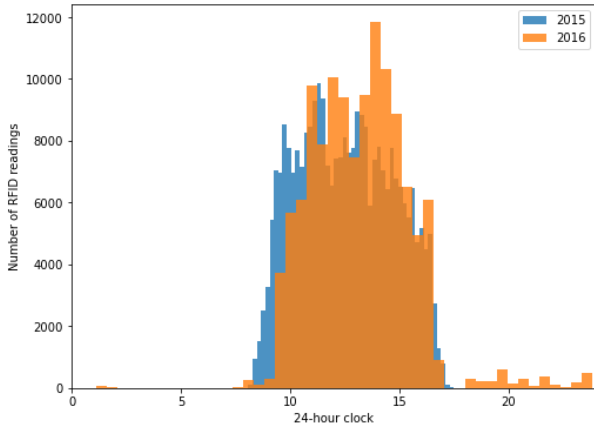


Fig. 3: **Sparrow data distribution during both seasons:** RFID readings recorded each day ranging from day 0 of the season to day 92 (season 1, 2015) and 88 (season 2, 2016).



**Fig. 4: Sparrow data distribution during both seasons:** Cumulative RFID readings recorded for each season during a day, plotted in a 24-hour format. The blue plot represents 2015 (season 1) and orange is 2016 (season 2).

Sparrows are diurnal birds, meaning they remain active and eat during the daytime [12]. Analysing the data, we obtain the expected distribution of landing times at the feeder during the day. The average distribution for all birds is shown in Fig. 4, in a 24-hour clock format.

This diurnal distribution may also be in part due to the habitual power outage of Lundy Island during some hours of the night when no feeder landings can be recorded. The irregular (few) data recordings at night were recorded towards the end of season 2, between days 87 and 92.

Almost all sparrow species eat their treats during this time. However, how often sparrows eat depends on their age and other demographic factors; as a result, slight variations in the landing frequency will be present, depending on the bird. Featherless young sparrows need to eat regurgitated food more frequently, while the feeding frequency of ageing sparrows reduces significantly [12].

#### IV. THEORY - THE MAKING OF A NETWORK

In its simplest form, a network is a collection of points, or nodes (vertices), joined with lines, or edges [13]. In our analysis, each node represents a bird. An edge is a social connection between two birds, which can be interchangeably called a friendship or a neighbour in a network. Social connections will be defined by two birds landing in the feeder within the same time window (see Section IV-B). The weight of the node, also called degree, is determined by the number of unique connections (friends) it has. Similarly, the weight of an edge represents the frequency of co-occurrence of the same connection. Weights visually correspond to the thickness of the network structure.

Throughout the project, we used the Python modules *Pyvis* [2] and *NetworkX* [14] to visualise, interactively manipulate and extract information from network graphs.

##### A. Landing times: "Alpha" ( $\alpha$ )

Birds can jump in and out of the feeder during a single seating. To determine the actual landing times of each sparrow,

we must account for this behaviour. We do this by introducing a new parameter, called alpha ( $\alpha$ ).

**Definition 1: Alpha** ( $\alpha$ ) is the minimum time of absence of a sparrow, for the next time it appears at the feeder (a new RFID reading) to be considered a new landing.

To explain this, for simplicity, take a bird landing twice, with a period of absence of 1s. If we set  $\alpha = 1$ s, the two landings will be considered a singular one, commencing at the initial landing. The period of absence for some birds will vary as a result. We can attempt to find a value of  $\alpha$  that best parametrises our data by looking at the variation of some network structures.

Fig. 5 summarises how this method works.

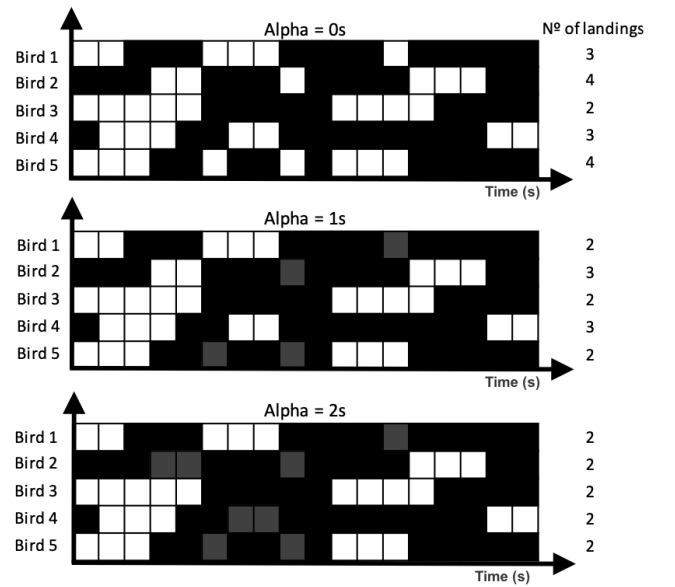


**Fig. 5: Landing time variation with alpha:** An example database of 5 birds over 18s. The black tiles represent the times when the bird is present in the feeder, a white tile is when it is absent. The grey tiles are filled presences in the feeder; used to remove artefacts from the data (treated as a black tile in the analysis). The first plot shows the landing times at  $\alpha = 0$ s, the second at  $\alpha = 1$ s and the last at  $\alpha = 2$ s. The variation in the resulting number of landings for each bird is also shown on the right.

##### B. Establishing Social Connections: "Beta" ( $\beta$ )

Birds are known to form clusters of organized groups, called flight flocks [3]. It is believed this is because it increases their odds of survival, as it increases the possibility of finding food and protecting each other from trouble and predators [11].

In a feeder, these social groupings can be extracted by analysing the proximity of birds landing [9] [10]. Given our fission-fusion model, we can set a maximum temporal separation between two birds' landings from each other that defines a connection, which we've called beta ( $\beta$ ).

**Definition 2: Beta** ( $\beta$ ) is the maximum landing time separation between two different sparrows to be considered a new connection/edge in our network (synchronous activity).

As an example, if two birds land at a feeder 10s apart. A value of  $\beta \geq 10$ s is needed for a connection to form in our network.

Fig. 6 summarises how the parameter  $\beta$  affects how connections form, and the shape of the resulting network.

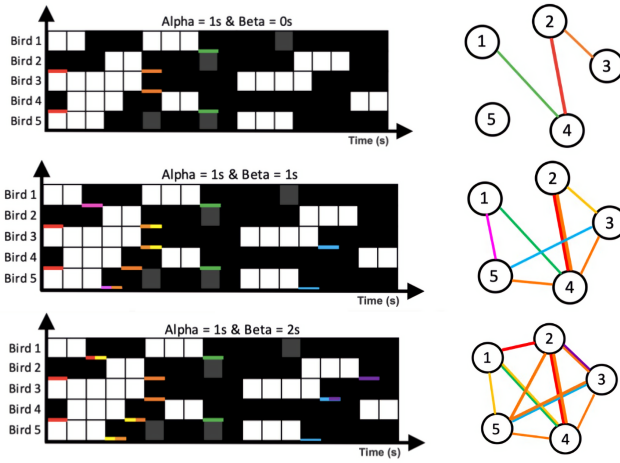


Fig. 6: **Connection formation variation with beta:** An example database of 5 birds over 18s. At a fixed value of  $\alpha = 1s$ . The first plot shows the connections formed at  $\beta = 0s$ , the second at  $\beta = 1s$  and the last at  $\beta = 2s$ . The time when a connection between two birds is formed, it's underlined with the same colour. The variation in the resulting network between the 5 birds is also shown on the right. This figure follows the same scheme as in Fig. 5.

## V. NETWORK ANALYSIS

A given network can be denoted as  $G = (V, E)$ , with  $|V|$  total nodes and  $|E|$  edges. A node  $u$  has friends denoted by  $v$ , these can also be called neighbours. The total number of friends of  $u$  is given by its degree,  $d(u)$ , without considering the number of times each friendship link is repeated (weight). Whenever the weight is considered, we denote the weighted degree as  $d_w(u)$ . Similarly,  $|E|_w$  denotes the sum of the weighted edges in the network.

### A. Average shortest path length

The Shortest Path length is a measure of the fastest way some information can reach another extreme of the network. The path length of a network is measured using Dijkstra's algorithm, which examines all the possible paths between a node  $u$  and its furthest reachable node  $v$ , using a min-priority queue that runs in time  $\mathcal{O}(|V| + |E| \log |V|)$  [15].

### B. Eccentricity

The eccentricity  $e_G(u)$  of a node  $u$  in a connected network  $G$ , is the maximum distance between  $u$  and  $v$ , over all nodes  $v \in G$  [16]. For a completely disconnected network, all nodes are defined to have infinite eccentricity.

Calculating the mean of all the eccentricities provides a measure of how the structure and connections of the network vary, as well as providing information when  $G$  starts to form sub-communities by disconnecting groups of components. In addition, the eccentricity is a value that can be compared inversely to the centrality of a network. The larger  $e_G(u)$  is, the less central  $u$  is in  $G$ .

### C. Community detection

Community detection in our network helps us reveal the hidden flocks among the nodes in the network. Many algorithms exist and mostly approach this as an optimisation problem, such as optimising the segregation of nodes based on their centrality measures (e.g. betweenness [17]).

In our investigation, we use an algorithm implementation that uses Clauset-Newman-Moore greedy modularity maximization [18] to find communities within  $G(u, v)$ . Optimisation of modularity over all possible partitions of the networks using simulated annealing or other external optimisation methods seemed impossible due to the computational effort required. Consequently, this method of community detection results in demonstrably higher quality than competing methods, in a shorter running time.

### D. Centrality as a Measure of Sociability

In a network, there are different ways to quantify the importance of a node. In this investigation, we have focused mainly on Eigenvector, Betweenness and Closeness centrality measures.

Each of these measures assesses the importance of the node by assuming and following different topological criteria.

#### 1) Betweenness

Betweenness centrality quantifies the importance of a node depending on the number of paths that must traverse through it if two other nodes want to be connected. This is a measure of how *in-between* the node is when information is spread through the network.

#### 2) Closeness

Closeness centrality indicates how close a node is to all other nodes in the network. It is calculated as the average path length (or geodesic distance) from the node to every other reachable node in the network [19].

#### 3) Eigenvector

Eigenvector centrality is a more sophisticated view of centrality. Unlike the others, it assumes that having more contacts is not the main criterion of importance, but instead, it ranks nodes more highly if they have more important contacts. Under this assumption, the centrality of a node is related to the sum of the centrality of its neighbours (connections) [20].

## VI. LOOKING FOR ALPHA AND A BETA

Various methods were investigated to attempt to find optimum values for  $\alpha$  and  $\beta$ . These are the values that will best describe the behaviour of the sparrows at the feeder.

### A. Bird patterns

Initially, the distributions of landing times with  $\alpha$  and  $\beta$  were explored. We explored the repeatability in the total number of landings per week, as we would expect bird sociability to remain fairly constant throughout the season, by minimising the difference between every other week. However, due to the highly variable data throughout the season, as seen in Fig. 3, this didn't seem appropriate. The significant peak in the number of landings in the feeder halfway through both

seasons could be because of the Christmas holidays when the farmer is likely bringing in more food into the feeder.

Alternatively, the variation in the number of landings times as a function of  $\alpha$  was plotted in both winters. This is shown in a log-log plot in Fig. 7. The trends in both seasons follow a similar relationship and overlap at around the same value of  $\alpha = 145 \pm 20$ s, when their trend becomes linear.

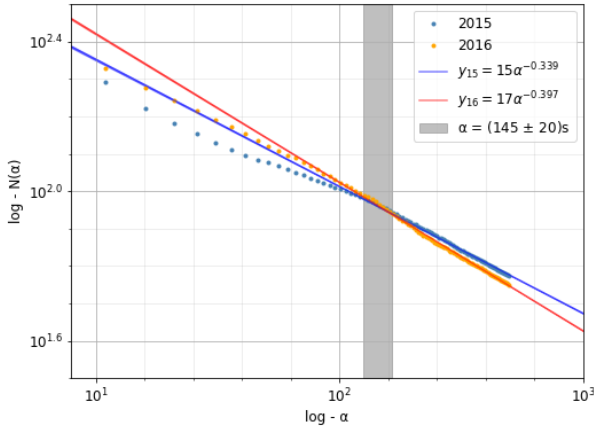


Fig. 7: Log-log plot of number of landing in both seasons: for different values of  $\alpha$  in the range [0,500]s. Both seasons overlap and commence a linear region at  $\alpha = (145 \pm 20)$ s.

A comparison of the number of landings of the 37 birds that are common in both winters was also visualised. Their percentage change ( $\Delta\%$ ) in the number of landings, at a fixed  $\alpha$  and  $\beta$  is plotted in Fig. 8. An initial idea was to minimise the mean  $\Delta\%$  for all birds. This wasn't explored further as bird behaviour changes as they age and have less need to feed, or are more prone to infections, disease, and being predated during the season.

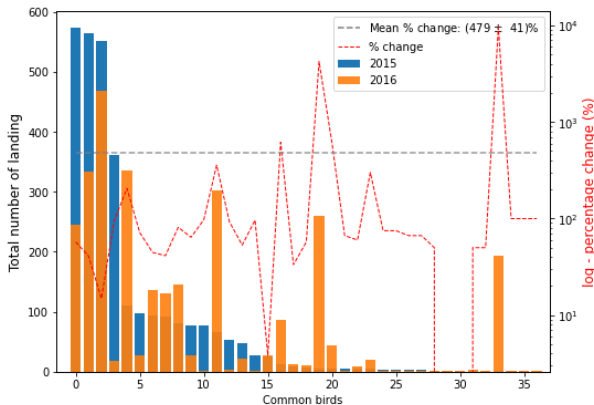


Fig. 8: Common birds feeder behavioural change: Number allocated to the common birds between both seasons, according to the sorted total number of landings in 2015 (plotted in blue). On the same left y-scale, 2016 is plotted in orange. The percentage change of the bird landings is shown in a red dashed line, plotted in a log-scale (right). The mean has also been calculated (in grey). Network parameters used  $\alpha = 210$ s and  $\beta = 90$ s.

### B. Variation in network measures

Alternatively, we considered how some network parameters and average bird centrality measures vary as we explored a range of  $\alpha$  and  $\beta$ .

We plot the variation of total number of edges  $|E|$ , average degree  $d(u)$ , eigenvector, betweenness and closeness centrality, in the initial (most variational) and interesting range of  $\alpha$  and  $\beta$  in [0, 60]s, this is plotted in Fig. 9. We find no interesting results as most show a smooth variation, with no discontinuous behaviour. The only chaotic plot is Eigenvector centrality; however, this becomes smoother at bigger temporal values. For larger  $\alpha$  and  $\beta$ , we find they all become even more uniform and vary less drastically with the same temporal increment, as the network is so interconnected at that point.

### C. Empirical considerations

Even though the initial part of the project was based on finding optimum values for these temporal parameters, we noticed that additional information and time would be needed to confidently define these values. Linear relationships, correlation patterns and overlaps between seasons cannot be used to specify temporal definitions, when factors such as age, predation and seasonal variation within others are not taken into account.

The sparrows in Lundy Island have been investigated for years. Ecology and biology PhDs have been carried out on this species. After inconclusive results on  $\alpha$  and  $\beta$ , and communication and footage evidence from [5] [6], we chose  $\alpha = 210$ s and  $\beta = 90$ s. These are empirically determined values and will be used for the rest of this investigation.

## VII. CORRELATIONS

We expect the pathway of influence transmitted by nodes that have a high centrality score in one measure to be correlated with their ranking in other centrality assessments. All of the nodes high in these measures can influence many other members of the network, either directly or indirectly facilitating or hindering other network connections.

We have found the correlations between the 5 network measures using a range of  $\alpha$  and  $\beta$  from [0, 250]s. We determine how the total number of edges  $|E|$ , the average degree  $d(u)$ , eigenvector, betweenness and closeness centrality measures vary with each other. This is visualised in a Pearson correlation heat map, in Fig. 10.

The maximum correlation was found among degree and closeness of  $0.997 \approx 1.0$  rounded to 2 significant figures. On the other hand, the measure with the smallest absolute correlations was Eigenvector centrality, due to its chaotic behaviour at small values of  $\alpha$  and  $\beta$ . Betweenness was found to have an inverse (negative) correlation with all other network parameters.

The average absolute correlation was found to be 0.68 with a standard deviation of 0.26, indicating that most correlations would be considered strong. The amount of correlation between degree, betweenness, closeness, and eigenvector indicates that these measures are distinct, yet conceptually related. These results are consistent with what is expected from

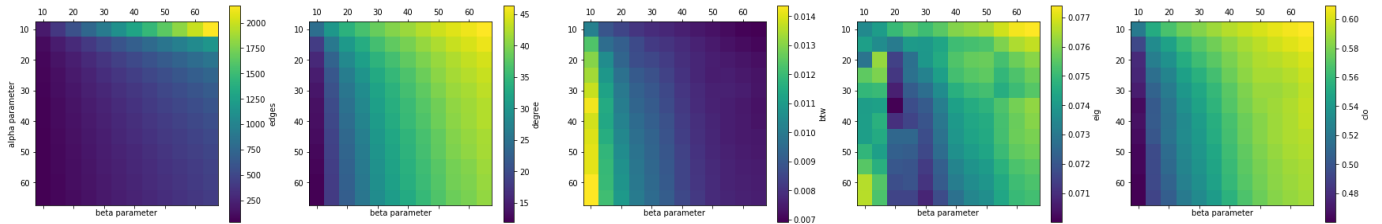


Fig. 9: **Centrality variation with  $\alpha$  and  $\beta$ :** Total number of edges  $|E|$  (1) and average centrality variation (Degree (2), Betweenness (3), Eigenvector (4) and Closeness (5)) plotted as a function of  $\alpha$  and  $\beta$  in the initial range of  $[0, 60]$ . This becomes more uniform at larger extremes.

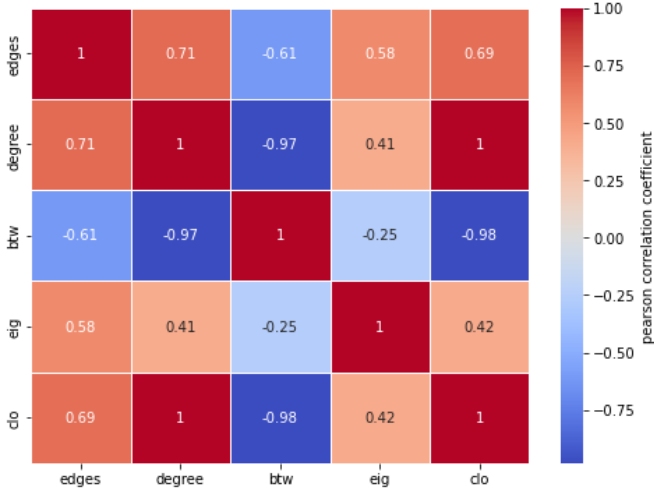


Fig. 10: **Pearson correlation map between network parameters:** Correlation map between total number edges  $|E|$ , the average degree  $d(u)$ , eigenvector, betweenness and closeness centrality. This plot is extracted by varying  $\alpha$  and  $\beta$  in the range of  $[0, 250]$ s.

these measures as seen in [21] and [22], where the average correlations were found to be around 0.7.

### VIII. POWERS LAWS

Power-law have been observed in many natural phenomena and have been investigated in a lot of depth [23] [24] [25]. If edges in the network were placed between nodes at random, the resulting degrees would follow a Binomial or Poisson distribution [13], with most nodes having degrees close to the mean value.

Networks, whose distributions follow some sort of power law, are now often referred to as scale-free [26], following Pareto distributions [24]. The precise term of a scale-free network varies, but it mainly comes if the fraction of nodes with degree  $x$  follows a power-law distribution of  $x^{-\gamma}$ , with  $\gamma > 1$  [25].

The distribution of degrees can be seen as the simplest measure that falls under this definition. As seen in Fig. 11, we can fit a simple power-law distribution of the form  $\sim Ax^{-\gamma}$  to both seasons. The observation of a power-law distribution thus indicates that the placement of edges in the network is, in a sense, far from being random. Nonetheless, these distributions don't follow power laws precisely. Some studies have also shown this in other networks. Nonetheless, they do tend to

have skewed degree distributions with a lot of low-degree nodes and a small number of high-degree hubs [27]. More predominant unevenness in the power-law description is seen in the data from 2015.

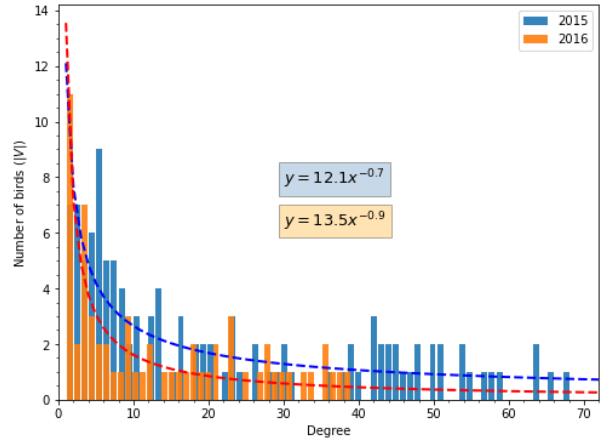


Fig. 11: **Degree distribution of network:** Node degree distribution of 2015 and 2016. Power laws are fitted to each season. network parameters used are  $\alpha = 210$ s and  $\beta = 90$ s.

The variation in the total number of edges  $|E|$  in a network is plotted against the average weighted degree,  $d_w = |E|w/|V|$ , as  $\beta$  is varied from  $[0, 120]$ s. The percentage difference from the maximum number of edges  $E_{max}$  a network with  $|V|$  nodes is calculated, using the theoretical maximum  $E_{max} = |V|(|V| - 1)/2$ . This is all shown in Fig. 12.

The figure shows two power-law distributions, at a similar  $\gamma$  factor for both seasons. The percentage difference seems to decay at an exponential rate, as the number of edges increases at a reducing rate with  $\beta$ .

With some particular fat-tailed power-law distributions, it is not uncommon to scale the bins, so the size of each bin goes up by a constant multiple. This is known as logarithmic binning [1].

Given the inspiration in Christensen et al. [23], we investigated periods of absence of each bird, from the feeder. In Fig. 13 we plot the variation in the number of birds that have a period of absence of more than the specified event size (s), in a log-log plot. The linear fit is also shown, where the most linear range has been used (determined by eye). Logarithmic binning is also implemented to improve the uneven distribution of birds at larger event sizes. This may be because of our small

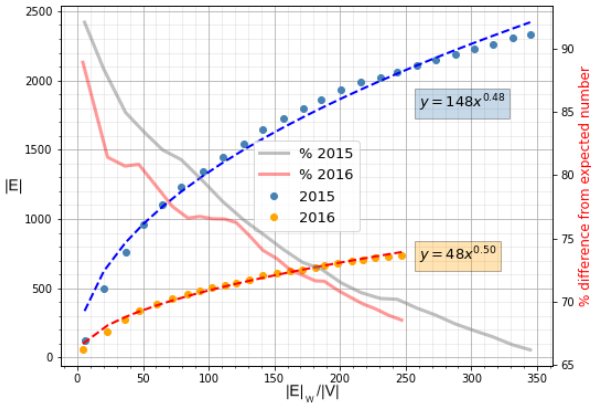


Fig. 12: **Variation of edge number with average degree:** The variation in the total number of edges  $|E|$  in a network is plotted against the average weighted degree,  $d_w = |E|_w/|V|$ . This plot is obtained by varying  $\beta$  in the range from  $[0, 120]$ s, at a fixed  $\alpha = 210$ s. The percentage difference from the maximum network connections ( $E_{max} = |V|(|V|-1)/2$ ) is also plotted in the secondary y-axis.

sample size of birds, where we are not expected to obtain a linear relationship [28].

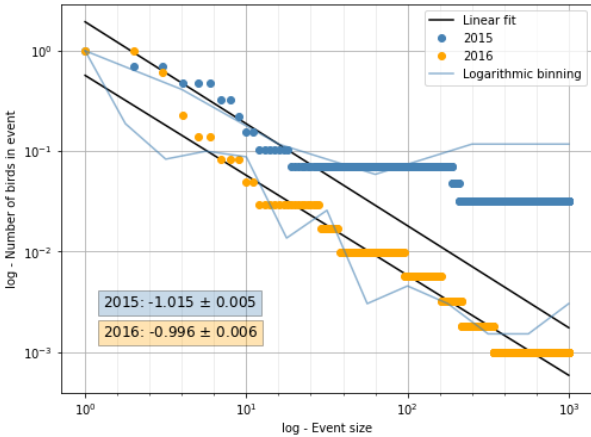


Fig. 13: **cumulative bird count for a period of absence:** Log-log plot of a cumulative distribution for the number of birds absent for more or equal to the event size ( $s$ ). The linear binning of data is plotted in blue for 2015 and orange for 2016. To compare both seasons, the bird count on the y-axis has been normalised. Logarithmic binning has also been implemented. The linear gradient extracted from both seasons is shown in a box, with its corresponding colour.

## IX. SPARISIFICATION METHODS

Sparsification methods provide a way of cleaning up unwanted edges from a network, which helps uncover the significant, hidden communities.

This Section explains all the sparsification methods that were considered in this investigation.

### A. Weakest connection

The first method was simply removing the weakest friendship link from each bird. For a given node  $u$  with edges to  $v$ ,

we remove the weakest friendship ( $v_{weak}$ ). Whenever a bird has more than one  $v_{weak}$ , the node removed is selected at random to reduce systematic errors that could introduce biases in selection.

A downside of this method is that it always isolates birds that only have one friend.

### B. Edge threshold

An alternative method is to filter and remove all edges in the network that have a weight below a certain threshold  $E_{th}$ .

This will significantly skew our network by only keeping the most central birds. These are the ones with more friendships and more co-occurrences per friendship.

### C. L-score

A local filtering score (l-score) for every edge can be calculated, using a logarithmic scale [29],

$$l_c(u, v) := \begin{cases} 1, & \text{if } d(u) = 1 \\ 1 - \frac{\log(r_c(u, v))}{\log(d(u))}, & \text{otherwise} \end{cases} \quad (1)$$

where  $l_c \in [0, 1]$ .

The nodes incident on  $u$  can be ranked according to their edge weight and given a score  $r_c(u, v)$  which is  $\leq d(u)^a$  where  $a \in [0, 1]$ , depending on its rank. Equation (1) can be used to calculate the corresponding l-score, where its value is high if the edge is important.

Given this score, a threshold  $l_{th}$  can be applied to remove any edges lower than this value. The edge will be removed only if the l-score is lower than the threshold, according to both nodes (i.e.  $l_c(u, v_i)$  and  $l_c(v_i, u) < l_{th}$ , where  $v_i$  is a particular neighbour  $v$  of  $u$ ).

Satuluri et al. [30] and Hamann et al. [29] observed a structure-preserving sparsification for low  $l_c$  thresholds. This allows edges to be more evenly distributed among the network, cleaning up very dense parts while maintaining sufficiently important weak edges. This is because, higher degree nodes have more incident edges below a certain  $l_c$  threshold, and lose more neighbours after filtering, however, they still keep more edges than lower degree nodes.

This method of sparsification prevents nodes from being completely isolated in our network, as at least one neighbour is always conserved. This is the first case in (1), where  $l_c(u, v) = 1$  when  $d(u) = 1$ . This may force the network into unnatural 'tree-like' structures at higher  $l_c$ -values, but provides a good method of edge cleanup for a network with varied distribution of node degrees.

### D. Expected connections

In a network, the expected edge weight between  $u$  and  $v$  is found using [31]

$$\langle E(u, v) \rangle = \frac{d_w(u) \cdot d_w(v)}{|E|_w}. \quad (2)$$

The ratio between the edge weight in our network to its expected value gives us the variance of this expected number

of connections. Where the square root gives the standard deviation ( $\sigma$ ),

$$\sigma = \sqrt{E(u,v)/\langle E(u,v) \rangle}. \quad (3)$$

For a given edge in a network, how many standard deviations away it is from its expected value is given by

$$N_\sigma = \frac{E(u,v) - \langle E(u,v) \rangle}{\sigma}. \quad (4)$$

The distribution of  $N_\sigma$  in our networks, for both seasons is plotted in Fig. 14. Approximating it to a normal distribution, the first season (2015) has a mean of  $\mu_{15} = -5.7$  and standard deviation of  $\sigma_{15} = 15.7$ . Similarly, the second season (2016) has  $\mu_{16} = -9.9$  and  $\sigma_{16} = 22.4$ . Connections above 1,2 and 3  $N_{\sigma 15/16}$  have approximately a significance level of 84.2%, 97.8% and 99.9%, as they represent the top 15.5%, 2.2% and 0.1% of the total network edges.

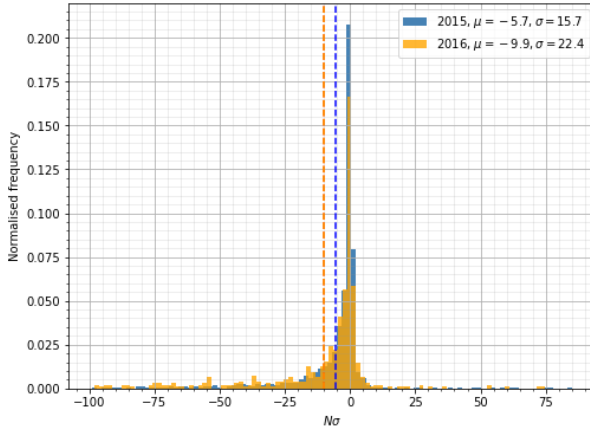


Fig. 14:  **$N_\sigma$  distributions for both seasons:** Normalised distribution of number of standard deviations above expected connections, given by (4).

The negative  $\mu_{15/16}$  could mean birds tend to be less friendly on average and only have a few important friendship connections. This could mean our data is overestimating the number of sparrow friendship links. Additionally, 2016 seems to comprise a larger spread of personality traits, with some birds being more friendly than expected, while others showing more dominant features. Nonetheless, this may be an artefact of the dataset in 2016 being smaller.

Given a network  $G(u,v)$ , we can filter and visualise edges that have an edge weight of  $N_\sigma$  above or below from its expected weight.

#### E. Repeated connections

The final sparsification method was based on analysing weekly networks, to assess the repeatability of friendships.

Some edges between nodes only appear in a single week of our data, while others can appear in more than half. A threshold can be set on the number of weeks a friendship connection must be present, for it to be classified as important. We can then create sub-networks with these filtered friendships, and these can be analysed and compared to other sparsified networks.

#### F. Network variation

##### 1) Ratio of kept edges

Fig. 15 compares how the ratio of kept edges varies for each sparsification method, in a log-log plot.

The L-score sparsification method gives the most similar filtering between both seasons, as it is a ranking against each network's nodes. In comparison,  $N_\sigma$  threshold provides the steepest variation, especially in season 2, possibly due to its more irregular degree distribution, as seen in Fig. 11.

For the edge thresholds, both seasons are plotted in different  $[min., max.]$  thresholds. Season 1 has a maximum of  $E_{max}(u,v) = 454$ , while season 2 requires a much smaller threshold to disconnect all the edges at  $E_{max}(u,v) = 298$ .

The weekly threshold filtering is varied from  $[0, 7]$ . It follows a very linear decrease in the log-log plot. For 2016, a steeper decrease is seen at the end, where it's likely the number of edges left drops more steeply than what was described by the previously power-law relationship.

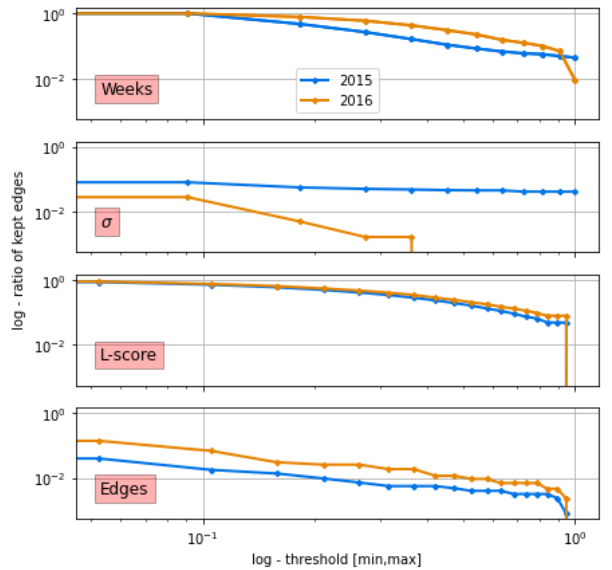
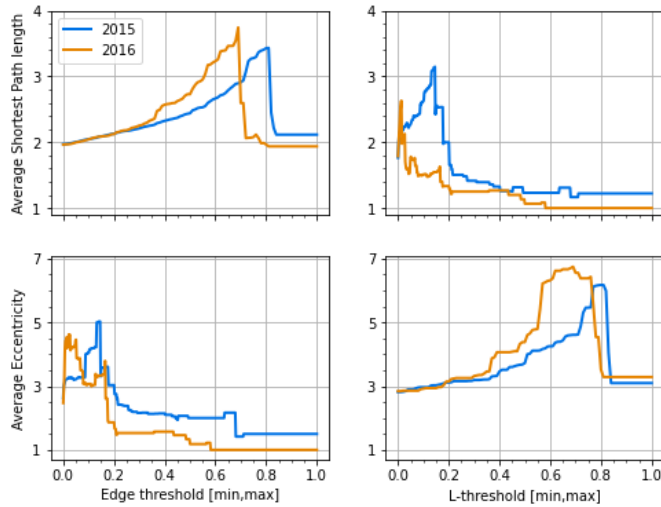


Fig. 15: **Sparsification methods comparison:** The ratio of kept edges plotted against a given threshold  $[min., max.]$  in a  $\log - \log$  plot for each sparsification method used (weekly,  $N_\sigma$ , L-score and edge threshold). The edge thresholds are varied from  $[0, 454]$  in season 1, and from  $[0, 298]$  in season 2. Weeks and  $N_\sigma$  are set to vary from  $[0, 7]$ , while L-score ranges from  $[0, 1]$ .

##### 2) Eccentricity and shortest path length

The variation in the average eccentricity and the Shortest path length of each of the 4 sparsification threshold, as they are increased from  $[min., max.]$  is plotted in Fig. 16 (Edge and L-score threshold) and Fig. 17 (weekly and  $N_\sigma$  significance threshold).

As the threshold is increased from  $[min., max.]$  in the network, the average shortest path length and eccentricity, peaks and then drops off. This is because all sparsification methods eventually disconnect nodes of the network and create separated communities. This significantly reduces the maximum distance (eccentricity) and the shortest path length between all connected nodes in a sub-graph. Nonetheless, be-



**Fig. 16: Network variation with threshold:** Edge threshold varied from  $[0, 454]$  (left) and L-score from  $[0, 1]$  (right). The average shortest path length and eccentricity are plotted against sparsification threshold.

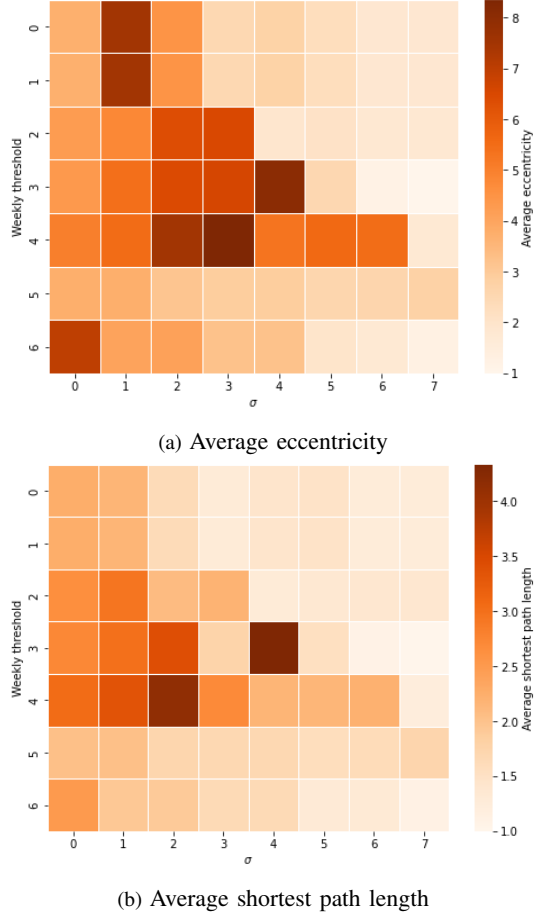


**Fig. 17: Network variation with threshold:** Weeks ( $y$ -axis) and  $N_\sigma$  ( $x$ -axis) are set to vary from  $[0, 7]$ . The average shortest path length (a) and eccentricity (b) are plotted against sparsification threshold.

fore these sub-graphs form, edges disappear and both distance measures increase.

These plots give us useful insight into how the network

Centrality	$\mu_{\sigma^2}$	$\sigma_\mu^2$	$\Delta(\sigma_\mu^2, \mu_{\sigma^2})$
Eigenvector	0.042	0.073	0.43
Closeness	0.063	0.078	0.19
Betweenness	0.016	0.031	0.49

**TABLE I: Centrality repeatability:** The centrality (eigenvector, closeness, betweenness) was calculated for each bird in every week it was present. The mean and variance of the centrality score was calculated for each bird,  $\mu$  and  $\sigma^2$  respectively. The mean of all the variances  $\mu_{\sigma^2}$  and the variance of all the means  $\sigma_\mu^2$  were found. The relative difference between both measures is presented under  $\Delta(\sigma_\mu^2, \mu_{\sigma^2})$ .

structure varies with each sparsification method. These distance measures peak at different points, depending on the threshold used and the measure being investigated. The second winter requires a lower threshold overall relative to the first, as it has fewer nodes.

## X. REPEATABILITY

We found significant repeatability in bird social measures by calculating the mean and variance of a bird's centrality scores on a weekly basis, over the two seasons. The mean of the variances ( $\mu_{\sigma^2}$ ) and the variance of the means ( $\sigma_\mu^2$ ) were found for each centrality measure. Our results are shown in Table. I.

The  $\mu_{\sigma^2}$  are smaller than  $\sigma_\mu^2$  in all cases. The most repeatable measure is betweenness centrality, presenting nearly  $\approx 49\%$  difference between  $\mu_{\sigma^2}$  and  $\sigma_\mu^2$ . The smallest is for closeness, at  $\approx 19\%$ . All these measures are significant at a significance level of above 10%, hinting at the immutability of bird social traits.

## XI. JACCARD SIMILARITY

The Jaccard similarity  $JS$  measures the similarity between two sets of data. It's calculated by dividing the number of observations in both sets by the number of observations in either set [32].

### A. Node comparison

The first Jaccard similarity method that was implemented scores the similarity between two nodes' immediate neighbourhood [29],

$$JS_n(u, v) = \frac{|N(u) \cap N(v)|}{|N(u) \cup N(v)|} = \frac{T_{uv}}{d(u) + d(v) - T_{uv}}, \quad (5)$$

where  $N(u)$  denotes all the neighbours of node  $u$ , and  $T_{uv}$  is the triangle's edge score; this is the number of 3 node triangle-networks an edge  $u, v$  belongs to.

When this method is used as a mode of comparison between two networks ( $G_1$  and  $G_2$ ), it compares the friendship links of the same bird ID and assigns a similarity value from  $[0, 1]$ . For a node that is not present in both networks, a value of  $JS_n = 0$  is appended to the list. The average and standard deviation of this list can be calculated, to find a final measure of the node similarity  $JS_n$  between the two networks.

### B. Edge comparison

An alternative Jaccard similarity method is comparing the similarity of all the friendship links, that are shared between both networks,

$$JS_e(G_1(E_1), G_2(E_2)) = \frac{|E_1 \cap E_2|}{|E_1 \cup E_2|}. \quad (6)$$

This method was allowed to run in two ways, by allowing the edge weight to be considered, or not.

If the weight is considered, the intersection between two edges that are equal to the minimum weight between both. If the weight is not taken into account, the intersection between two identical edges will always be one. Alternatively, if the edges are not the same, their intersection is 0. An overview of the algorithm is written in pseudocode, as follows:

**Run  $JS_e$  with Weight = True or False**

```

if  $E_1 = E_2$  then
    if Weight = True then
         $|E_1 \cap E_2| = \min(|E_1|, |E_2|)$ 
    end if
    if Weight = False then
         $|E_1 \cap E_2| = 1$ 
    end if
end if
Else  $|E_1 \cap E_2| = 0$ .
```

## XII. DESCRIBING OUR NETWORK

### A. Threshold comparison: most significant connections

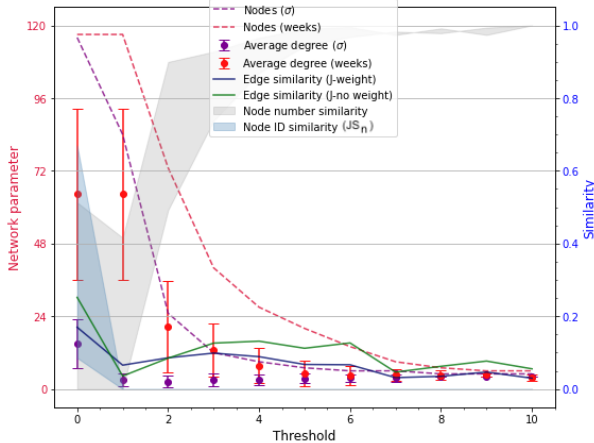


Fig. 18: **Network variation with weekly, and  $N_\sigma$  thresholds:** Plot showing variation of network parameters as the threshold of  $N_\sigma$  and weeks is increased from [0, 10]. network parameters plotted are the number of nodes and average degree in the network. Also plotted on the secondary axis is the variation in the Jaccard similarity for node ID friendships ( $JS_n$ ) and total edges ( $JS_e$  with and without weight). These are (5) and (6) respectively. The similarity in node number between both networks after the threshold is applied is also shown. This plot is for both seasons (2015 and 2016) combined.

We attempt to find values for how often friendship groups vary in sparrows, by looking at the weekly variation of connections (weekly threshold) and how significantly different the friendship connections are to a purely theoretical network ( $N_\sigma$  threshold).

We plot the variation of the number of nodes and the average degree of the network as we increase each of these thresholds from [0, 10] in Fig. 18. We notice the similarity between our networks, across all our Jaccard measures, drops, as each of these thresholds increases, meaning each method filters connections significantly differently. In the same figure, we plot the node number similarity between both networks. This value increases as both networks lose a significant number of nodes at higher threshold values.

Fig. 19 shows the variation of the similarity between networks filtered with either weekly and  $N_\sigma$  thresholds, as a heat map. Comparing the weighted edge (6) and node (5) in Fig. 19a and 19b respectively. In addition, we also look at their similarity by considering how much correlation there is between the network centrality distributions. A similar approach has been investigated by Soundarajan and Eliassi in [33]. However, in their approach, they lose the identification of nodes. We keep this and only compare the sparrows present in both networks. This is shown in Fig. 19c.

From Fig. 19b and 19a, we notice that according to our  $JS$ , our sparrow networks seem to be most similar at a  $N_\sigma = 0$  threshold (the expected number), and in the ones containing connections appearing in at least  $3 \pm 1$  weeks in either season.

The correlation plot is not considered to a large extent (Fig. 19c) as this is directly dependent on the number of nodes present, where the correlation between very few birds seems to carry a high correlation at  $N_\sigma = 7$  and weeks = 5, making it inadequate to extract any conclusions from it. Nonetheless, it corroborates our results with the higher correlation present for low  $N_\sigma$  and weekly threshold  $> 2$ .

### B. Comparison: weeks and seasons

In Fig. 20, we plot the variation of the edge similarity ( $JS_e$ ) on a week-by-week comparison, throughout both seasons. As expected, all the diagonals have a value of  $JS_e = 1$ .

At first sight, comparing both seasons (top-right and bottom-left sections) have the lowest  $JS_e$  on average. As a mode of direct comparison, when we calculate the mean friendship similarity between the 37 nodes that overlap in both seasons, we find a low average value of  $JS_n = (0.145 \pm 0.056)$ .

Additionally, the elements closest to the diagonal have the largest  $JS_e$  values. This could justify our reasoning to think that bird friendships are maintained for more than a week and vary after a certain number of weeks. To quantify this repetition of the friendships of our network between weeks, we find the distance of the maximum value in each row, from the diagonal. The mean and standard deviation of this value is calculated to be  $\mu_r = 2.22$  and  $\sigma_r = 1.85$ , where the subscript  $r$  denotes repeatability. Given our sample size, at 1.96 standard errors in the mean, we find  $\mu_r = 2.22 \pm 0.70$ . We can conclude that the repetition of friendships occurs in the range of 1 week and 4 days, to 2 weeks and 6 days, at a 95% significance level.

### C. Flock size: Community detection

We attempt to analyse the variation of the number of flocks (communities) as we vary different sparsification thresholds,

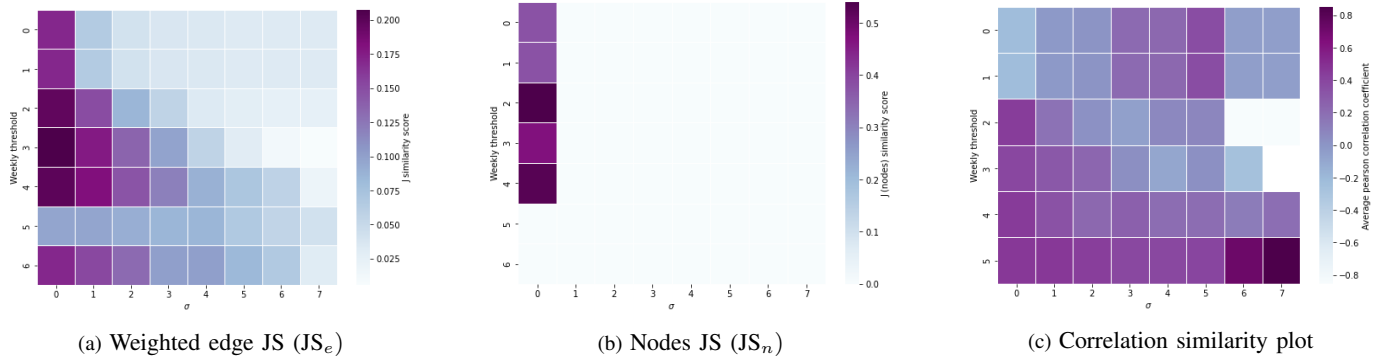


**Fig. 19: Network similarity with threshold sparsification:** Variation in the correlation and JS (nodes (5) and weighted edge comparison (6) with Weekly repetition (from [0, 6]) and  $N_\sigma$  significance (from [0, 7]) threshold, in the vertical and horizontal axis. These plots are for both seasons (2015 and 2016) combined.

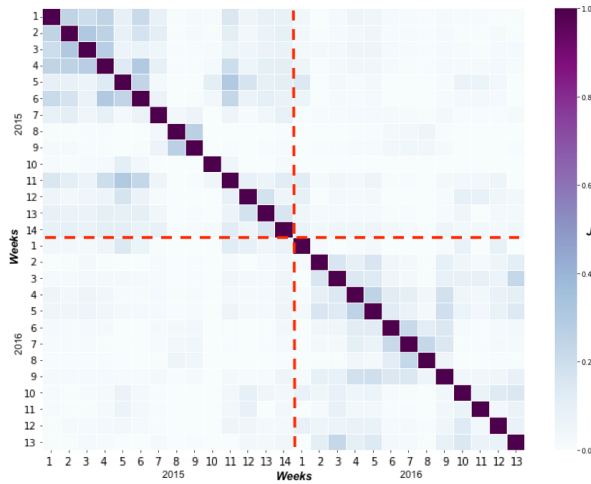


**Fig. 20: Week-by-week similarity:** Heat map showing the Jaccard edge similarity ( $JS_e$ ) variation on a week-by-week comparison, for both seasons. The dashed red lines represent where one season ends and the other starts.

such as: L-score, Weekly and  $N_\sigma$  threshold. The resulting heat maps for each of these are plotted in Fig. 21.

Increasing the L-score threshold forms more sub-networks and communities, as the network forms more branching structures at its higher values.

A visual representation on how the network changes can be seen in the Appendix E.

If the number of sparrow communities on the Island was known, such as the usual number of friends each bird feeds with, we could find threshold parameters that optimise the number of flocks. From Fig. 21c, if we optimised for the largest number of sparrow communities on the smoother, we would expect sparrow friendships to vary on a weekly/bi-weekly basis. These connections have a threshold of  $N_\sigma = 1$  from the expected, where only the top 15.8% of the edges of the original network have been kept.

### XIII. SIMULATED NETWORKS

We propose three different randomised network models, to study the importance of interactions and connections in our sparrow's feeder data. Each method is randomised differently

and carries a different amount of information from the original network.

#### 1) Method 1 - Conserve Bird Landing Number

The first random method uses the times from the sparrow feeder data, scrambled and distributed non-uniformly to each node, according to their landing frequency. We will denote this method as C.N.

The centrality of birds is close to being conserved. Most friendship links between the highly central birds will be kept, as these are the ones that visit the feeder the most.

#### 2) Method 2 - Don't Conserve Bird Landing Number

The second method is similar to method 1. However, in this case, each bird is allocated the same number of landing times as every other bird. We will call this method d.C.N.

This will completely scramble the significance of each node in the network and the centrality measures of most birds will likely change. This is the most random simulated network.

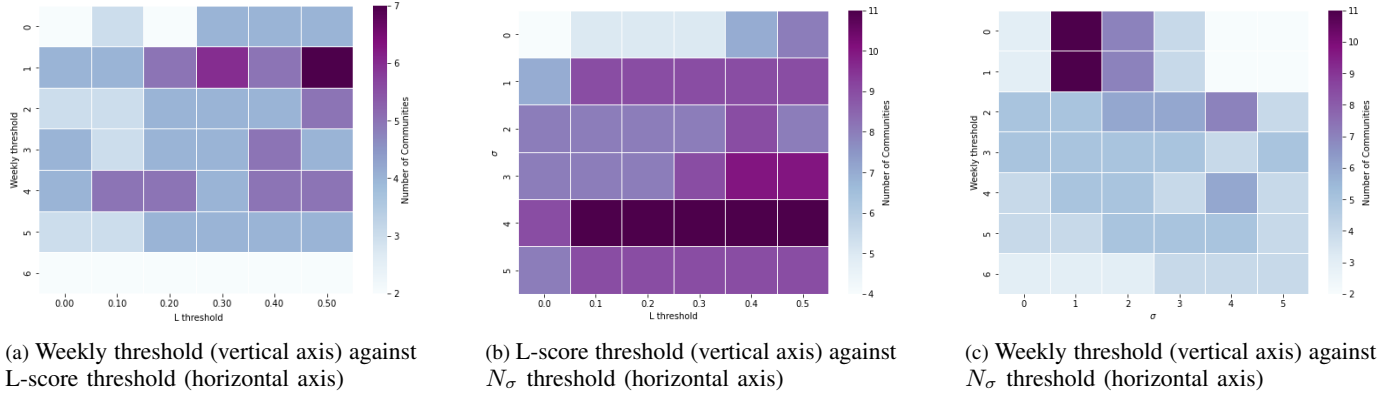
#### 3) Method 3 - Distribute Bird Landing Numbers

The third and last random method doesn't use any of the individual RFID readings but instead uses the diurnal and seasonal distribution of bird landings (these are fits to Fig. 4 and 3). We will refer to this method as D.N.

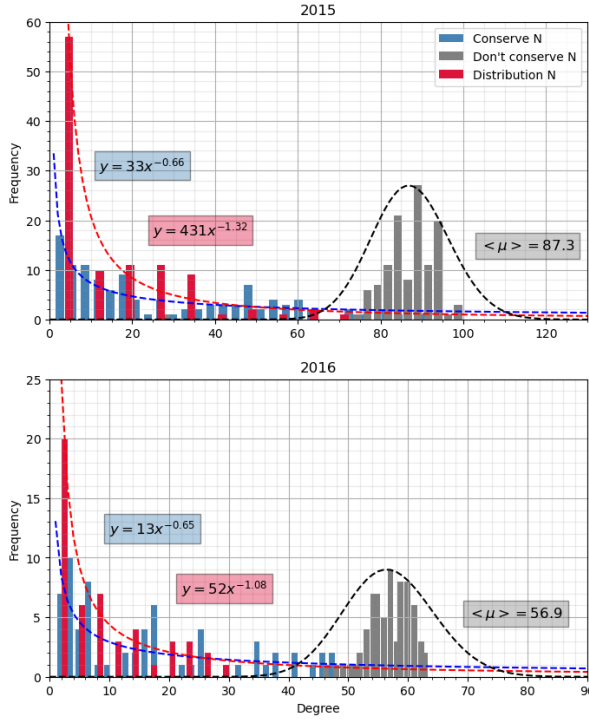
This method provides the most adequate representation of a simulated sparrows network as we should expect their behaviour to follow these landing distributions, however, we have completely erased any possible friendship links and weekly repetition.

Fig. 22 shows how the node distribution varies with degree. As we'd expect, the most random network (Method 2 - d.C.N.), follows an approximately Poisson distribution with average degree  $\langle \mu \rangle$  and width  $\langle \mu \rangle^{1/2}$ . This is because a random allocation of degrees, on average, will give the majority of the birds the mean of those values. However, due to our small network size of  $|V| \approx 10^2$ , we see this follows a binomial distribution more closely. Nonetheless, in the case where  $\langle \mu \rangle \gg |V|$ , the binomial is well approximated by a Poisson distribution [34].

On the other hand, method 1 (C.N), follows a more uniform, slower decreasing power law, relative to method 3 (D.N) and our network (see Fig. 11). Nonetheless, this still indicates that some nodes of different sizes coexist in the network.



**Fig. 21: Variation in number of communities using NetworkX package with sparsification thresholds:** L-score [0,0.5], weekly repetition [0,6] and Standard deviation ( $N_\sigma$ ) [0,5] significance. In these plots, both sparsification thresholds are applied to the same network, and its communities are analysed.



**Fig. 22: Degree distribution for all three random methods:** Plot showing the power law distributions followed by method 1 (conserving landing number) and 3 (distribution of landing times). However, method 2 (not conserving landing number) follows a binomial  $\approx$  poisson distribution, a sign of a purely random network [34]. This is an average over 5 runs of the simulated networks, to decrease the noise. This is shown for both seasons.

#### A. Comparison

To compare all three random methods to our network, we analyse the  $JS_n$  (Table II), weighted  $JS_e$  (Table III, IV) and results from statistical tests comparing centrality similarity (Fig. 23).

In 2015, Table III, the mean of the weekly comparisons for C.N. lies  $1.87\sigma$  below the mean of the data. Similarly, dC.N and D.N. lie  $4.97\sigma$  and  $2.72\sigma$  away for season 1. These represent a significance level of 3.04%,  $3.4 \times 10^{-5}\%$

and 0.33%, for C.N., dC.N and D.N. respectively. The same analysis is not carried out for season 2 (Table IV) as the standard deviations are much larger, due to the smaller dataset. From season 1, we can conclude to a significance level of  $< 5\%$ , that the weekly mean repeatability of the random networks ( $\mu_{C.N.}, \mu_{dC.N.}, \mu_{D.N.}$ ) is not as or more repeatable than our data ( $\mu_{Data}$ ). Additionally, the most random method (dC.N.) has the lowest values for all parameters in  $JS_e$  ( $Max.$ ,  $\mu$ ,  $\sigma$ ).

From Table II we see low  $\mu$  and highly spread ( $\sigma$ ) values for  $JS_n$ . It has an expected highest value for  $JS_n$  when the landing times for each bird are conserved, as the central birds still visit the feeder the most in the simulated network, and hence are more likely to create similar friendship links. D.N. and dC.N. reassuringly show significantly lower similarity values. The  $p$ -value of these results is  $\ll 1\%$ , meaning that it is very unlikely that our sparrow friendships can be replicated through randomly simulated networks, even when information on their daily feeding distribution is retained.

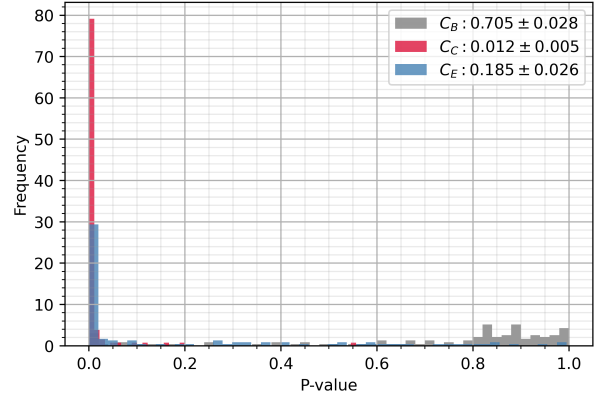


**Fig. 23: P-value histogram:** Histogram showing the distribution of  $p$ -values for all three centrality measures: Betweenness ( $C_B$ ), closeness ( $C_C$ ) and eigenvector ( $C_E$ ). This plot has been extracted by comparing the 100 randomised trials for D.N. against our data. The mean and standard error for each centrality measure is given in the legend ( $\mu_i \pm \sigma_{\mu_i}$  with  $i = E, B, C$ ).

Finally, to compare our last random method (D.N.) against

TABLE II:  $JS_n$ 

Method	$\mu$	$\sigma$
Data	1.0	0.0
C.N.	0.32	0.22
d.C.N.	0.25	0.18
D.N.	0.20	0.17

TABLE III:  $JS_e$  2015

	Max.	$\mu$	$\sigma$
	1.0	0.18	0.24
	0.45	0.075	0.056
	0.27	0.016	0.033
	0.34	0.044	0.050

TABLE IV:  $JS_e$  2016

	Max.	$\mu$	$\sigma$
	1.0	0.13	0.25
	0.41	0.082	0.091
	0.20	0.024	0.041
	0.42	0.057	0.079

TABLE II, III, IV: **Similarity comparison between our data and all 3 random methods:** Conserve landing number (C.N.), don't conserve landing number (d.C.N.), and using the distribution of landing number (D.N.), over 100 runs. All our results are presented to 2 significant figures. Table II shows the  $JS_n$  between our data and the method (in the first column) on a weekly basis, for both seasons combined. The average of all the week node similarity scores ( $\mu$ ) and its standard deviation ( $\sigma$ ) is calculated. Table III and IV show similar results for  $JS_e$  but separated into both seasons, 2015 and 2016 respectively, and additionally gives the maximum weekly edge similarity (Max.).

our data, we perform a  $\chi^2$ —squared test for each bird's centrality ( $C_i$  with  $i = E, B, C$ ) among the 100 trials. The distribution is plotted in Fig. 23. We find for both  $C_E$  and  $C_C$ , the mean  $p$ -values with associated errors of the mean are  $p_E = 0.18 \pm 0.03$  and  $p_C = 0.012 \pm 0.005$ . Meanwhile,  $C_B$  has  $p_B = 0.70 \pm 0.03$ . This means  $> 99\%$  of the time, our randomised method will produce significantly different bird closeness centrality measures for all birds. For eigenvector centrality, we still find an abundance of low  $p$ -values, however, not significant enough to be able to conclude they are significantly different. Betweenness shows very spread results with larger  $p$ -values.

Further analysis should be carried out regarding this method of comparison. Nonetheless, the average centrality differs between the randomised network and our data. This implies that we are not able to completely replicate identical bird sociality given the general social distribution and behaviour of sparrows at a feeder.

#### XIV. A BRIEF LOOK INTO DOMINANCE AT THE FEEDER

Fig. 14 shows that on average, sparrows tend to have fewer connections than expected. This could mean they potentially have very few close friendships. Given the same filtering criteria as in Section IX-D, we rank and keep the top 10 birds with the lowest  $N_\sigma$  away from the expected number of connections. These are listed in Table V.

##### A. Elo ranking

The Elo-rating method can be used to infer dominance hierarchies based on ranking [6]. This is obtained from a temporal sequence of directed interactions, recorded as a sequence of 'winner' and 'loser' nodes. Birds with the most wins will have the highest rating and are identified as the most dominant.

This method is directly dependent on the total pool of birds against which they are ranked. Nonetheless, we should expect a negative correlation between  $N_\sigma$  and Elo-rating, as birds with a higher tendency to be dominant in one group should also be perceived as dominant in another group, repeating their social traits (see Section X).

BirdID	$N_\sigma$	$\Delta N_\sigma$
8730	-1125.8	354.3
8586	-193.1	417.4
8608	-185.0	590.9
8465	-95.2	249.0
8434	-70.6	213.2
8710	-61.9	172.0
8486	-59.9	221.5
8480	-54.2	135.8
8652	-41.9	145.5
8448	-38.7	149.2

TABLE V: **List of top 10 most dominant birds in our dataset:** Sparrows ranked by lowest  $N_{\sigma}$  away from the expected number of connections.

For the birds that we have Elo-ratings for [5] [6] and are also present in our time-series data, we can plot the variation in the calculated  $N_\sigma$ -significance against elo-rating. This is shown in Fig. 24.

We analysed the correlation and found a slight negative Pearson correlation of  $r = -0.058$ . However, the error in this value is  $\approx 300\%$ . This may be due to the limited data we are sampling, making this analysis insignificant and inconclusive.

##### B. Sex-dominance relationship

To test the relationship between sex and dominance, we compare our dominance rank to a sex spreadsheet from [5]. This spreadsheet has a limited number of Bird IDs, with only 80 birds for which roughly all of them have a  $N_\sigma = 0$  in our network.

We don't have data for the top 10 most dominant birds in Table V. This may be because usually, ornithologists wait until juveniles and females grow to record their sex, as it's hard to identify their sex visually when they are very young. These sometimes die before they moult into their adult plumages.

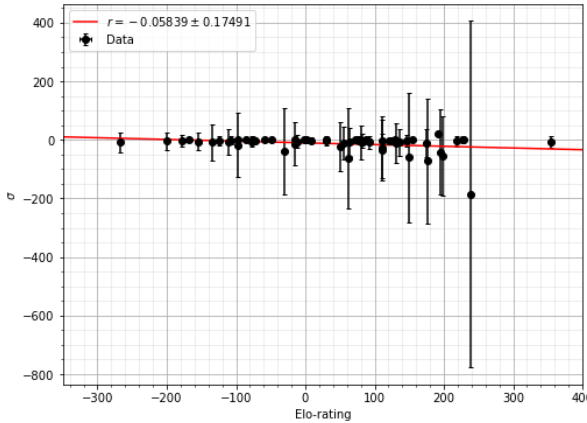


Fig. 24: **Dominance method comparison:** Plot of elo- and  $N_\sigma$ -rating. The errorbars represent the standard error in the mean ( $N_\sigma$ ).

Nonetheless, we believe no definitive conclusions can be extracted from the dominance list, as it is very unlikely that either extreme in life span dominates the feeder. Instead, we propose studying this further, with more conclusive data.

## XV. DISCUSSION AND CONCLUSIONS

In this investigation, we have analysed and visualised networks of time series RFID data, from a sparrow feeder in Lundy Island, a small Island off the North Devon coast of the UK. We have done this by introducing temporal parameters to identify sparrows' landings, and how they form connections. We have considered sparrows that synchronising activities such as foraging, to be considered in the same social grouping.

We have analysed centrality measures, network dimensions and communities within the sparrow network. Additionally, we have created sparsification methods to identify the most important connections in the network: by removing the weakest edge from each node, filtering edges under a certain weight, edges below a certain logarithmic rank (l-score), filtering above certain standard deviations above the expected number of connections and removing friendships that don't appear on a weekly basis. Additionally, the expected connections method allows us to extract a list of the most dominant birds at the feeder, by looking at those that differ the most. We compare this method to Elo-ratings and have found no significant correlation.

We have also implemented methods to find the similarity between networks. By finding the Jaccard similarity of node friendships, or the total edges, and by looking at the centrality measures correlation between the same bird in each network.

Observing the maximum similarity between weeks, we have compared the edges present in a week with every other week in our data. We calculate the distance the maximum similarity from that week is away from its direct comparison (i.e. diagonal elements in a heat map). Doing this, we find mean weekly repeatability of 2 weeks and 2 days with a margin of error of  $\pm 4$  days, at a 95% significance level. We have found that optimising for the maximum number of communities corroborates these results - a significance level of  $1\sigma$  above the expected number of connections.

Additionally, we find correlations between network centrality measures: betweenness, closeness and eigenvector, as well as total network edges and node average degree, and find an average of 0.68 with a standard deviation of 0.26. This agrees with what has been reported from similar studies.

Finally, we compare our network to 100 trials of 3 different simulated random networks (each retaining a different proportion of information from the original data). We find that it's very unlikely that random networks have a similar weekly repetition of  $> 2$  weeks, with a  $p$ -value of less than 1%, indicating a significance of the friendship connections in our network. Additionally, given the landing behaviours of sparrows through the day and season, centrality measures were found to be significantly different with a minimum mean  $p$ -value of  $0.012 \pm 0.005$ .

Nonetheless, this investigation is far from complete. In addition to the factors we have investigated, more data should be analysed, such as birds' age, predators, diseases, and the environment that can contribute to any alteration to their lifespan and, hence, feeding patterns. Additionally, bird behaviour in the feeder, such as the jumping in and out, can be dependent on other factors. For example, a bird may jump more if there are dominant birds present in the feeder, or if they are more juvenile. Further investigations could take these aspects into account, by analysing the network with variable temporal parameters.

## APPENDIX A NETWORK ANALYSIS

*NetworkX* was used for the creation, manipulation, and study of the structure, dynamics, and functions of complex networks [14]. It's written completely in Python which makes the code easy to read and understand, before implementing it into our methods. *Scipy*, *Numpy* and *Pandas* were used for the data analysis section. *Matplotlib*, *Pyvis* and *NetworkX* were used for graph and network visualisations.

## APPENDIX B NETWORK DIMENSIONS

### A. Average shortest path length

Given this shortest length  $\text{dist}_G(u, v)$ , the average shortest path length ( $L_G$ ) over all nodes in the network is found using

$$L_G := \frac{\sum_{u,v \in V(G)} \text{dist}_G(u, v)}{|V|(|V| - 1)}. \quad (7)$$

The diameter is the largest geodisic distance corresponding to a network. However, this measure is less useful for real networks than the average shortest distance since it only measures the distance between one pair of vertices at the end of the distribution of distances.

### B. Eccentricity

The eccentricity  $e_G(u)$  of a node  $u$  in a connected network  $G$ , was found using

$$e_G(u) := \max \{ \text{dist}_G(u, v) : v \in V(G) \} \in \mathbf{N} \cup \{\infty\}. \quad (8)$$

### C. Community detection - maximising modularity

The modularity is, up to a multiplicative constant, the number of edges falling within groups minus the expected number in an equivalent network with edges placed at random [35]. Many real-world networks are sparse and hierarchical, in which case this algorithm runs in essentially linear time  $\mathcal{O}(|E|\log^2|V|)$ .

Greedy modularity maximization begins with each node in its separate community and joins the pair of communities that most increases modularity until no such pairs exist [14].

### APPENDIX C

#### CENTRALITY MEASURES

##### A. Betweenness

Given the total number of geodisic that link two nodes  $v_1$  and  $v_2$  is  $g_{v_1 v_2}$ , while the number of those that include node  $u$  is  $g_{v_1 v_2}(u)$ . The Betweenness centrality of node  $u$  is the ratio of these, given by [36],

$$C_B(u) = \sum_{v_1, v_2} \frac{g_{v_1 v_2}(u)}{g_{v_1 v_2}}. \quad (9)$$

Where this sum is over all nodes in the graph and  $v_1 \neq v_2 \neq u$ .

##### B. Closeness

Closeness centrality is calculated using the average path length from the node to every other reachable node in the network [19]. This can be calculated using

$$C_C(u) = \frac{\sum_{v \in V(G)} g_{uv}}{|V| - 1}. \quad (10)$$

##### C. Eigenvector

The adjacency matrix of a graph  $G(u, v)$  is denoted by  $A = (a_{u,v})$ . This encodes all the information on node interconnections with every other node. The eigenvector centrality for the nodes  $u$  in the network is the solution  $x$  of the eigenvector equation

$$Ax = \lambda x, \quad (11)$$

where  $\lambda$  is a non-zero constant eigenvalue.

If the graph is strongly connected (ie. matrix  $A$  is irreducible), then  $x$  is unique and positive [37]. As a result, through Perron–Frobenius theorem we can find the positive solution  $x$  if  $\lambda$  is the largest eigenvalue of the adjacency matrix  $A$ . This can be solved using the power method, where repeatedly computing the eigenvector will make the solution converge to the most dominant eigenvalue and eigenvector [38].

The eigenvector centrality  $C_E(u)$  of node  $u$ , is given by the  $u$ th component of the vector  $x$ ,

$$C_E(u) = x_u = \frac{1}{\lambda} \sum_v a_{v,u} x_v. \quad (12)$$

### APPENDIX D

#### $P$ -VALUES AND $\chi^2$ -TEST

The reduced  $\chi^2$  value is calculated using

$$\chi_r^2 = \frac{\chi^2}{N_{dof}} = \frac{1}{N_{dof}} \sum_{i=1}^n \frac{(O_i - \lambda_i)^2}{\lambda_i}, \quad (13)$$

where  $\lambda_i$  and  $O_i$  are the are the expected and observed values respectively [39]. The number of degrees of freedom is given by  $N_{dof} = N_{runs} - 1$ , where  $N_{runs}$  is the number of simulated runs in this investigation.

A  $p$ -value can be obtained from the  $\chi_r^2$  value using

$$p\text{-value} = 1 - CDF(\chi^2) = 1 - \frac{\int_{\chi_{\min}/2}^{\infty} t^{\frac{N_{dof}}{2}-1} e^{-t} dt}{\int_0^{\infty} t^{\frac{N_{dof}}{2}-1} e^{-t} dt}. \quad (14)$$

### APPENDIX E

#### NETWORK STRUCTURE VARIATION

Fig. 25, 26, 27 show visually how the structure of the network varies, as we change  $N_\sigma$  and L-score, weekly and L-score, and weekly and  $N_\sigma$  thresholds respectively.

#### ACKNOWLEDGMENT

I'm grateful for the underlying support from my project partner, Dariusz Duszynski. Additionally, I would like to thank Jammie Dunning, Alex Chan [5] and Tim Evans [31] for our interesting conversations and contributions in our meetings. They have provided significant valuable analytical and ecological insight into sparrow behaviour and networks, a completely new topic for us at the start of this project.

#### REFERENCES

- [1] T. Evans, “Network notes,” complexity and Networks Course, Level 3 course. (PHYS96008) Physics Department, Imperial College London.
- [2] G. Perrone, J. Unpingco, and H. Lu, “Network visualizations with pyvis and visjs,” *CoRR*, vol. abs/2006.04951, 2020. [Online]. Available: <https://arxiv.org/abs/2006.04951>
- [3] M. MAYNTZ. What's a flock of birds called? understanding this behavior in birds. [Online]. Available: <https://www.thespruce.com/flock-names-of-groups-of-birds-386827>
- [4] T. Anderson, “Biology of the ubiquitous house sparrow: From genes to populations,” in *BofUHS. Print ISBN: 9780195304114*. Oxford Scholarship, 2006. [Online]. Available: <https://oxford.universitypressscholarship.com/view/10.1093/acprof:oso/9780195304114.001.0001/acprof-9780195304114-chapter-8>
- [5] J. Dunning, 01.2022 - 04.2022, Email and Microsoft teams meetings [Online].
- [6] A. Sánchez-Tójar, “The evolution of social dominance in house sparrows,” Ph.D. dissertation, Universität Konstanz, Konstanz, 2018.
- [7] S. Amsler and S. Shea. Rfid (radio frequency identification). [Online]. Available: <https://www.techtarget.com/iotagenda/definition/RFID-radio-frequency-identification>
- [8] M. C. S. C. Burley, N., “Social preference of zebra finches for siblings,cousins and non-kin.” *Anim. Behav.*, vol. 39, p. 775–784, 1990.
- [9] C. G. Casinello, J., “Spatial association in a highly inbred ungulate population: evidence of fine-scale kin recognition.” *Ethology*, vol. 114, p. 124–132, 2008.
- [10] C. L and R. T. J., “Activity synchrony and social cohesion: a fission-fusion model,” p. B.2672213–2218, 2000.
- [11] Z. Tóth, V. Bokony, A. Lendvai, K. Szabó, Z. Pénzes, and A. Liker, “Whom do the sparrows follow? the effect of kinship on social preference in house sparrow flocks,” *Behavioural processes*, vol. 82, pp. 173–7, 07 2009.

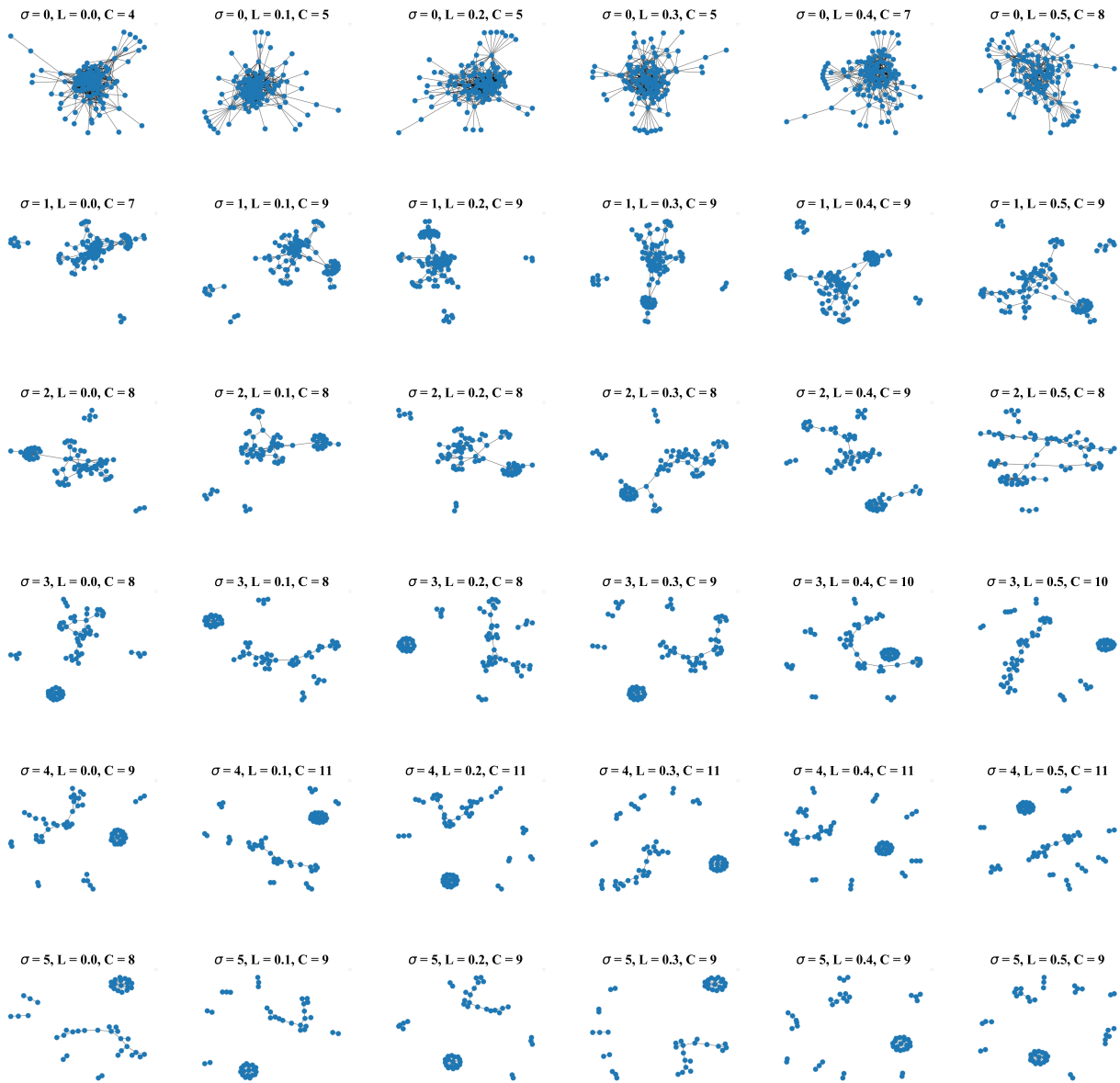


**Fig. 25: Season 1 network structure variation:** By varying the significance threshold of  $N_\sigma$  above the expected mean and the L-score of a given connection, less-significant connections are lost and the network structure changes (the number of communities ( $C$ ) varies). Variation of L-score in the range of [0,0.5] along the horizontal axis and  $N_\sigma$  of [0,5] in the vertical axis. This has been created using *NetworkX*.

- [12] K. Nadim. What do sparrows eat? a complete guide of feeding sparrows. [Online]. Available: <https://www.birdsadvice.com/sparrows-eat/>
- [13] M. Newman, "The physics of networks," *Physics Today*, vol. 61, pp. 11–33, November 2008.
- [14] M. Franceschet, "Eigenvector centrality," department of Mathematics and Computer Science. University of Udine. [Online]. Available: <https://www.sci.unich.it/~francesc/teaching/network/eigenvector.html>
- [15] P. Frana, "An interview with edsger w. dijkstra," *Communications of the ACM*, vol. (8) 53, p. 41–47, August 2010.
- [16] R. S. Z. Y. Matjaž Krnc, Jean-Sébastien Sereni, "Eccentricity of networks with structural constraints," *Discussiones Mathematicae Graph Theory, University of Zielona Góra*, vol. (4) 40, p. 1141–1162, August 2020.
- [17] M. E. J. Newman and M. Girvan, "Finding and evaluating community structure in networks," *Phys. Rev. E*, vol. 69, p. 026113, Feb 2004. [Online]. Available: <https://link.aps.org/doi/10.1103/PhysRevE.69.026113>
- [18] M. E. J. Newman, "Fast algorithm for detecting community structure in networks," *Phys. Rev. E*, vol. 69, p. 066133, Jun 2004. [Online]. Available: <https://link.aps.org/doi/10.1103/PhysRevE.69.066133>
- [19] J. Golbeck, "Chapter 3 - network structure and measures," in *Analyzing the Social Web*, J. Golbeck, Ed. Boston: Morgan Kaufmann, 2013, pp. 25–44. [Online]. Available: <https://www.sciencedirect.com/science/article/pii/B9780124055315000031>
- [20] P. Bonacich, "Power and centrality: A family of measures," *American Journal of Sociology*. [Online]. Available: <http://www.leonidzhukov.net/hse/2014/socialnetworks/papers/Bonacich-Centrality.pdf>
- [21] L. C. C. E. Valente TW, Coronges K, "How correlated are network centrality measures?" *Connect (Tor)*, vol. 28(1), pp. 16–26, Jan 1 2008.
- [22] F. Grando, D. Noble, and L. C. Lamb, "An analysis of centrality measures for complex and social networks," in *2016 IEEE Global Communications Conference (GLOBECOM)*. IEEE, dec 2016. [Online]. Available: <https://doi.org/10.1109%2Fglocom.2016.7841580>
- [23] O. Peters, C. Hertlein, and K. Christensen, "A complexity view of rainfall," *Physical review letters*, vol. 88, p. 018701, 02 2002.
- [24] A. Charpentier and E. Flachaire, "Extended scale-free networks," 2019. [Online]. Available: <https://arxiv.org/abs/1905.10267>
- [25] A. D. Broido and A. Clauset, "Scale-free networks are rare," *Nature Communications*, vol. 10, no. 1, mar 2019. [Online]. Available: <https://doi.org/10.1038%2Fs41467-019-08746-5>
- [26] D. J. de Solla Price, "Networks of scientific papers," *Science*, vol. 149, no. 3683, pp. 510–515, 1965. [Online]. Available:

- <https://www.science.org/doi/abs/10.1126/science.149.3683.510>
- [27] L. A. N. Amaral, A. Scala, M. Barthélémy, and H. E. Stanley, "Classes of small-world networks," *Proceedings of the National Academy of Sciences*, vol. 97, no. 21, pp. 11 149–11 152, 2000. [Online]. Available: <https://www.pnas.org/doi/abs/10.1073/pnas.200327197>
- [28] M. Newman, "Power laws, pareto distributions and zipf's law," *Contemporary Physics*, vol. 46, no. 5, pp. 323–351, sep 2005. [Online]. Available: <https://doi.org/10.1080%2F00107510500052444>
- [29] L. G. M. H. e. a. Hamann, M., "Structure-preserving sparsification methods for social networks," *Soc. Netw. Anal. Min.*, vol. 6, p. 22, April 2016.
- [30] V. Satuluri, S. Parthasarathy, and Y. Ruan, "Local graph sparsification for scalable clustering," in *Proceedings of the 2011 ACM SIGMOD International Conference on Management of Data*, ser. SIGMOD '11. New York, NY, USA: Association for Computing Machinery, 2011, p. 721–732. [Online]. Available: <https://doi.org/10.1145/1989323.1989399>
- [31] T. Evans, 01.2022 - 04.2022, Weekly in-person Supervisor meetings.
- [32] F. Karabiber, "Jaccard similarity," ph.D. in Computer Engineering, Data Scientist. Associate Professor of Computer Engineering. [Online]. Available: <https://www.learndatasci.com/glossary/jaccard-similarity/>
- [33] S. Soundarajan, T. Eliassi-Rad, and B. Gallagher, "A guide to selecting a network similarity method," in *SDM*, 2014. [Online]. Available: <https://pubs.siam.org/doi/10.1137/1.9781611973440.118>
- [34] A. L. Barabasi, "Network science, random networks." 08.09.2014. [Online]. Available: <https://barabasi.com/f/624.pdf>
- [35] M. E. J. Newman, "Modularity and community structure in networks," *Proceedings of the National Academy of Sciences*, vol. 103, no. 23, pp. 8577–8582, 2006. [Online]. Available: <https://www.pnas.org/doi/abs/10.1073/pnas.0601602103>
- [36] L. C. Freeman, "A set of measures of centrality based on betweenness," *Sociometry*, pp. 35–41, 1977.
- [37] M. Franceschet, "Eigenvector centrality," department of Mathematics and Computer Science. University of Udine. [Online]. Available: <https://www.sci.unich.it/~francesc/teaching/network/eigenvector.html>
- [38] M. Scott and P. Dauncey, "Computational physics notes - year 3 course," Imperial College London, December 2021-2022.
- [39] P. M. René Andrae, Tim Schulze-Hartung, "Dos and don'ts of reduced chi-squared," max-Planck-Institut für Astronomie, Königstuhl 17, 69117 Heidelberg, Germany.

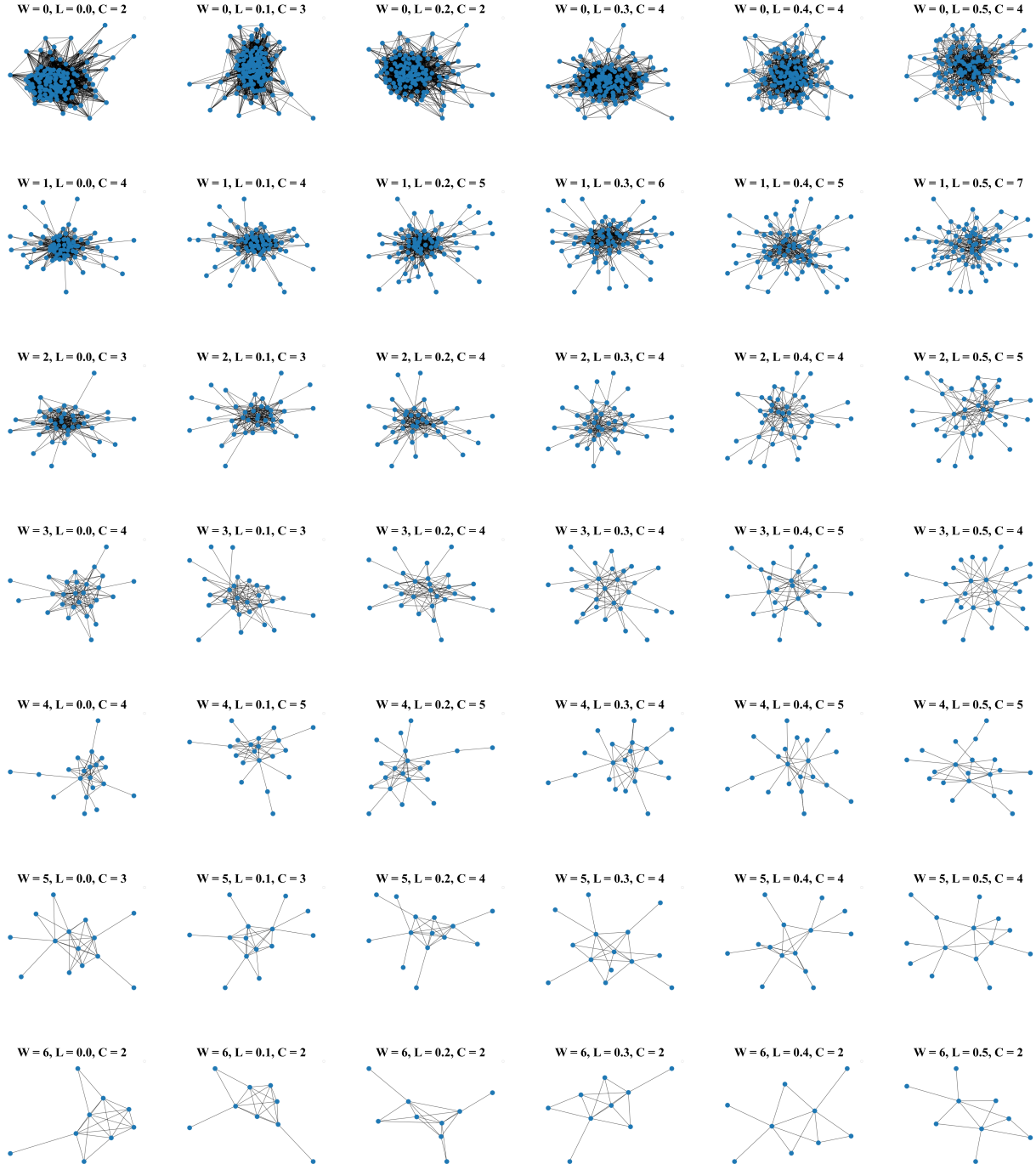


Fig. 26: **Season 1 network structure variation:** By varying the Weekly threshold ( $W$ : the number of weeks a given connection has to appear to be considered significant) and the L-score of a given connection, less-significant connections are lost and the network structure changes (the number of communities ( $C$ ) varies). Variation of L-score in the range of [0,0.5] along the horizontal axis and  $W$  of [0,6] in the vertical axis. This has been created using *NetworkX*.

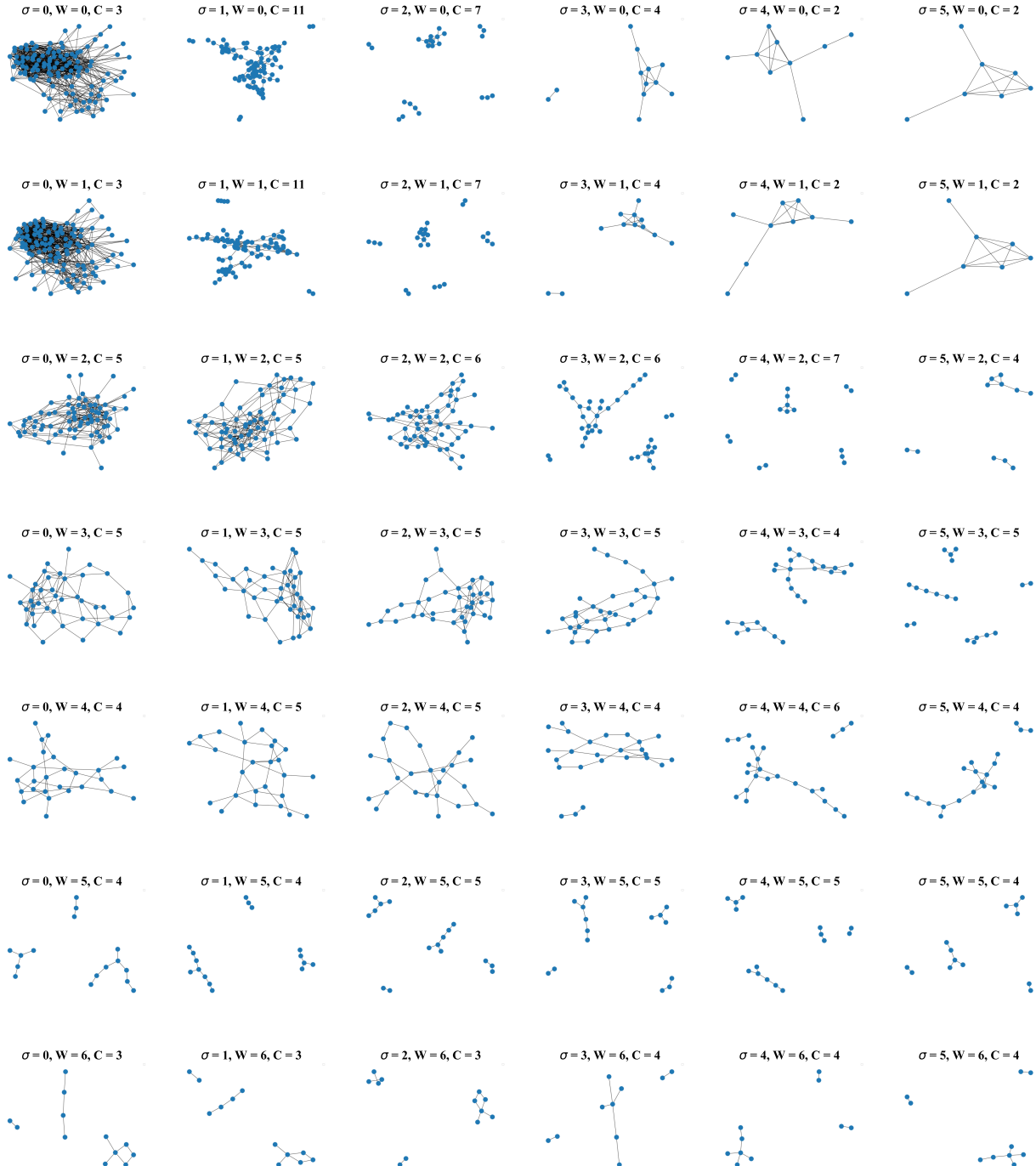


Fig. 27: **Season 1 network structure variation:** By varying the Weekly threshold ( $W$ : the number of weeks a given connection has to appear to be considered significant) and the the significance threshold of  $N_\sigma$  above the expected mean of a given connection, less-significant connections are lost and the network structure changes (the number of communities ( $C$ ) varies). Variation of  $N_\sigma$  of [0,5] along the horizontal axis and  $W$  of [0,6] in the vertical axis. This has been created using *NetworkX*.